Nanoscale

Accepted Manuscript

This is an *Accepted Manuscript*, which has been through the RSC Publishing peer review process and has been accepted for publication.

Accepted Manuscripts are published online shortly after acceptance, which is prior to technical editing, formatting and proof reading. This free service from RSC Publishing allows authors to make their results available to the community, in citable form, before publication of the edited article. This *Accepted Manuscript* will be replaced by the edited and formatted *Advance Article* as soon as this is available.

To cite this manuscript please use its permanent Digital Object Identifier (DOI®), which is identical for all formats of publication.

More information about *Accepted Manuscripts* can be found in the **Information for Authors**.

Please note that technical editing may introduce minor changes to the text and/or graphics contained in the manuscript submitted by the author(s) which may alter content, and that the standard **Terms & Conditions** and the **ethical guidelines** that apply to the journal are still applicable. In no event shall the RSC be held responsible for any errors or omissions in these *Accepted Manuscript* manuscripts or any consequences arising from the use of any information contained in them.

View Online

Cite this: DOI: 10.1039/c0xx00000x

www.rsc.org/nanoscale

PAPER

Nanoparticles assembled by aptamers and crystal violet for arsenic(III) detection in aqueous solution based on a Resonance Rayleigh scattering spectral assay

Yuangen Wu,[a,b] Shenshan Zhan,[a] Haibo Xing,[a] Lan He,[a] Lurong Xu[a] and Pei Zhou*[a]

Received 6th June 2012, Accepted Xth XXXXXXXXX 20012
DOI: 10.1039/b000000x

Aptamers assembled nanomaterials have captured much attentions from the field of analytical chemistry in recent years. Although they have been regarded as a promising tool for heavy metal monitor, the report involved in aptamers based biosensor for arsenic detection is rare. Herein we developed a highly sensitive and selective aptamer biosensor for As(III) detection based on a Resonance Rayleigh scattering (RRS) spectral assay. Prior to As(III) detection, we firstly assembled a variety of nanoparticles with different size *via* controlling the concentration of arsenic-binding aptamers in crystal violet (CV) solutions. The results of photon correlation spectroscopy (PCS) and scanning probe microscope (SPM) testified that the introduction of As(III) indeed had change the size of nanoparticles, which caused the great variation of RRS intensity at 310 nm. In the presence of 100 ppb As(III), the maximum decline ratio of RRS intensity was achieved for large nanoparticles assembled by 200 nM of aptamers and CV molecules, where the average size of nanoparticles had decreased from 273 nm to 168 nm. In the case of small nanoparticles, the maximum increase ratio of RRS intensity was obtained when the concentration of aptamer was over 600 nM. Combined with a RRS spectral assay, an effective biosensor has developed for As(III) detection, using above large and small nanoparticles as target recognition element. The present biosensor has a detection limit as low as 0.2 ppb, a dynamic range from 0.1 ppb to 200 ppb, and high selectivity over other metal ions. Such efficient biosensor will play an important role in environmental detection.

1. Introduction

Arsenic in drinking water is becoming a major public health issue in many regions worldwide.[1] Although arsenic exists in many different chemical forms in nature, it is found almost exclusively as arsenite (As(III) as H_3AsO_3) and arsenate (As(V) as H_3AsO_4) in water.[2] As(III) was identified as one of the most harmful substances in water to human health, and it is 60 times more toxic than As(V) or organic arsenic compounds.[3] Considering its high toxicity, the U.S. EPA and the WHO had reset the maximum contaminant level (MCL) for arsenic in drinking water from 50 to 10 ppb in 2001.[4] This lower MCL also promoted research to develop new methods for monitoring arsenic. Current popular methods for arsenic detection require sophisticated equipment and a long analysis time,[5, 6] so they are neither readily available in developing countries nor capable of on-site field detection. To overcome these problems, some novel chemosensors and biosensors had been developed.[4, 7] For example, Ray and co-worker developed a highly sensitive sensor for arsenic detection with a detection limit of 3 ppt using a dynamic light scattering assay.[8] Others used genetically modified *E. coli* cells and presented a pH-based biosensor for detection of arsenic in drinking water.[9] Recently, some fluorescence and quantum dots sensor has also been employed to monitor As(III).[4, 10] However, these methods usually needed some reactions or modification, thus they may be susceptible to the surrounding conditions. Therefore, it is highly necessary to develop simple and stable methods to detect trace As(III) in the environment.

Aptamers are single-strand RNA or DNA oligonucleotides with unique conformations that can distinctly bind to a broad range of targets, including small molecules, proteins, and even whole cells.[11, 12] Because aptamers are stable, high selective and cost-effective,[13] they have been used as components for many novel biotechnological applications, such as in diagnostics,[14] molecular imaging,[15] nanomaterial assembly,[16, 17] targeted therapeutics and drug delivery.[18, 19] Although a larger number of aptamer based biosensors have been developed for various metal ions detection with high sensitivity and selectivity,[20-22] the report involved in arsenic detection using aptamer as recognition

[a] *Key Laboratory of Urban Agriculture (South), Ministry of Agriculture, and School of Agriculture and Biology, and School of Environmental Science and Engineering, and Bor S. Luh Food Safety Research Center, Shanghai Jiao Tong University, Shanghai, 200240, China. Fax: +86-21-34205762; Tel: +86-21-34205762; E-mail: zhoupei@sjtu.edu.cn*
[b] *School of Chemistry and Chemical Engineering, Guizhou University, Guiyang, 550025, Guizhou, China. Fax: +86-851-4732925; Tel: +86-851-4732861*

element is rare. Recently, we have developed a novel colorimetric biosensor for As(III) with a detection limit of 5.3 ppb,[23] based on the aggregation of gold nanoparticles mediated by cationic polymers and aptamers.

Resonance Rayleigh scattering (RRS) spectral assay is simple, rapid and sensitive, and has been applied to the analysis of proteins, nucleic acids, inorganic ion, based on the simple molecular interaction between analytes and small molecules such as dye.[24, 25] Some inorganic nanoparticles such as Au and Ag exhibit good RRS effect, so they were usually used as an essential part of sensors for the RRS assay.[26, 27] Recent studies also indicated that some organic dyes can be applied to the determination of trace amount substances.[28, 29] Triphenylmethane (TPM) dyes, such as crystal violet (CV) and malachite green (MG), contain three phenyl rings and one positive charge, so that they can bind to DNAs through various noncovalent interactions including electrostatic force, base stacking force and coordinate bond. Previous works have testified that TPM dye could be used as a potential fluorescent reporter when it binds to aptamer,[30, 31] G-quadruplex and some supramolecules.[32, 33] The special interaction between TPM dyes and DNAs can be used for signal transduction in the design of aptamer based biosensor. Herein we assembled a variety of nanoparticles with different size by CV molecules and Ars-3 aptamers, and used them as recognition elements to develop an effective biosensor for As(III) detection based on a RRS spectral assay. The sensing system is very simple and it just contains Ars-3 aptamers and CV molecules, as illustrated in Scheme 1. In the presence of As(III), the size of large nanoparticles was decreased, which caused a decline of RRS intensity at 310 nm; while the diameter of small nanoparticles was increased and led to the enhancement of RRS intensity. The variation of RRS intensity was depended largely on the size alteration of nanoparticles that conditioned directly by As(III) concentrations, thus this signaling mechanism makes it possible to detect As(III) by a RRS spectral assay.

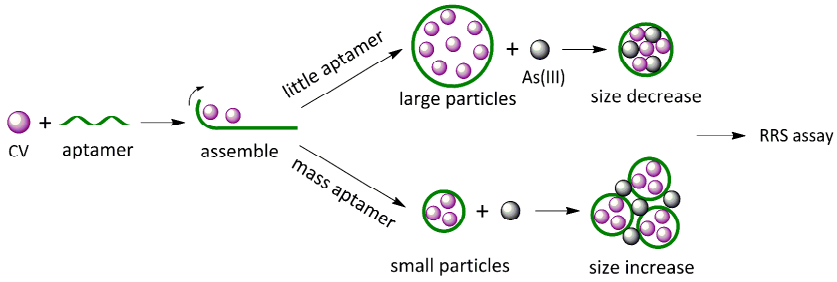

Scheme 1 Illustration of the biosensor for As(III) detection based on the size alteration of nanoparticles assembled by aptamers and CV.

2. Experimental

2.1 Chemicals and materials

The sequence of Ars-3 aptamer is reference to the previous literatures,[34] and was synthesized by Sangon Biotechnology Co., Ltd. (Shanghai, China). Its sequence is 5'-GGTAATACGACTCACTATAGGGAGATACCAGCTTATTCAATTTTACAGAACAACCAACGTCGCTCCGGGTACTTCTTCATCGAGATAGTAAGTGCAATCT-3'. Before use, the arsenic-binding aptamer was dissolved in 50 mM N-(2-hydroxyethyl) piperazine-N-2-ethane sulfonic acid (HEPES) buffer solution of pH 7.2. Crystal violet (CV) and malachite green (MG) were obtained from Sigma-Aldrich (Milwaukee, WI, USA). Methyl violet (MV), ethyl violet (EV), $SbCl_3$ and $BiCl_3$ were purchased from Sinopharm Chemical Reagent Co., Ltd. (Shanghai, China). Unless otherwise mention, all other reagents were analytical grade and used without further purification or treatment. Ultrapure water (Milli-Q plus, Millipore Inc., Bedford, MA) was used throughout.

2.2 Instrumentation

A model of F-4500 fluorescence spectrophotometer (Hitachi, Japan) was used to record the RRS intensity, with the excited slit of 10 nm and emission slit of 2.5 nm, and PMT voltage of 700 V. Circular dichroism (CD) spectra were collected with the J-815 Circular Dichroism Spectropolarimeter (Jasco, Japan) in HEPES buffer (50 mM, pH 7.2) to characterize the structure change of aptamers at room temperature. The optical chamber (0.5mL volume) was utilized. The scanning speed was 100 nm per minute. The CD spectra were collected in the range of 200-400 nm. Multimode Nanoscope IIIa scanning probe microscope (SPM) (Digital Instrument Inc., NY. USA) was used to observe the images of nanoparticles, and the procedure for samples pre-treatment is reference to our previous report.[28] The average size of nanoparticles was determined by photon correlation spectroscopy (PCS) (Malvern Instruments, UK).

2.3 Procedure of As(III) determination

An appropriate volume of 10 μM As-binding aptamer and 1 mM CV stock solution were added into a 2 mL plastic tube, diluted to 495 μL with ultrapure water. Then a 5 μL $NaAsO_2$ solution (As^{III}) with varying concentration was added, mixed thoroughly and incubated for 10 min. The blank sample was added 5 μL ultrapure water instead $NaAsO_2$ solution. The RRS spectra were recorded by means of synchronous scanning excited wavelength λ_{ex} and emission wavelength λ_{em} (λ_{ex}-λ_{em}=$\Delta\lambda$=0) on the fluorescence spectrophotometer. The RRS intensity at 310 nm (I) and the blank solution without $NaAsO_2$ (I_0) were recorded. The value of $\Delta I = [I - I_0]/I_0$ was calculated. To test the selectivity of the biosensors, methyl arsenic acid (MMA), dimethyl arsenic acid (DMA) and other metal salts including Na_2HAsO_4 (As^V), $SbCl_3$, $BiCl_3$, $Pb(NO_3)_2$, $Hg(NO_3)_2$, $Cd(NO_3)_2$, $AgNO_3$, $CaCl_2$, $ZnCl_2$, $FeCl_3$, $MgSO_4$, $MnSO_4$, $NiSO_4$, $CuSO_4$ and $FeSO_4$ were used.

3. Results and discussion

3.1 Nanoparticles assembled by aptamers and CV

To study the interaction between arsenic-binding aptamer and CV molecules, the varying concentration of Ars-3 aptamer was added into 100 μM of CV solution, and the RRS intensity at 310 nm was recorded. As shown in Fig. 1(a), the RRS intensity enhanced obviously with the increasing concentration of aptamer, and it reached the maximum at 400 nM of Ars-3 aptamer in CV solution. Fig. 1(b) confirms that only the coexistence of aptamer with CV in solution can enhance the RRS intensity obviously, which demonstrates that the possible interaction between As(III) and CV or aptamer will not interfere the RRS assay.

The great enhancement of RRS intensity indicated that Ars-3 aptamer had interacted with CV molecules to assemble CV-aptamer particles (complex). The process of particles assembly is presented in Scheme 2(a). Each CV molecule carries one positive charge and a three-phenyl ring, so it can bind to Ars-3 aptamer *via* the electrostatic force between its positive charges and negative charges of phosphate backbone in DNAs. The three-phenyl ring makes CV molecules hydrophobic, thus some of them will cluster each other to form a single-layer of lipoid liked micelle structure, where the hydrophilic parts with positive charges distribute on the surface and the hydrophobic parts are enclosed in the inner micelle. Therefore, it is highly feasible to assemble nanoparticles using electronegative aptamers and CV micelles with dense positive charges.

The interactions between aptamers and some other cationic TPM dyes were also investigated. The four cationic TPM dyes contain the same core (a three-phenyl ring), and the difference among them lies in their substitutent moieties (Fig. 1(c)). As shown in Fig. 1(d), the RRS intensities were apparently related to the substitutent moieties of cationic TPM dyes. MV and MG molecules have the asymmetric dimethylamino substituents, which would lead to instability in the assembly of nanoparticles. In particular, MG contains only two dimethylamino substituents, so the binding site for aptamer is less than other cationic TPM dyes. These reasons can explain why the RRS intensity in MG-aptamer solutions was the lowest one. In the case of EV solutions, the variation of RRS intensity is similar with that of CV solutions, but its value is less than the latter. Compared with CV molecule, EV molecule has the longer side groups and will occupy a larger space, which may hinder the assembly of nanoparticles to some extent. Therefore, the proper length and symmetry of side groups are critical to assemble nanoparticles. Regarding these two special features, CV molecules may be the most suitable cationic dyes for assembling nanoparticles.

The electrostatic force between CV molecule and Ars-3 aptamer plays a vital role in the assembly of nanoparticles. In general, the electrostatic force is associated with the ionic strength of solutions. Herein, the varying concentrations of NaCl were added into CV solutions to regulate its ionic strength during the assembly of nanoparticles. As shown in Fig. 1(e), the RRS intensity decreased gradually with the increasing of media ionic strength, and it attained the minimum at highest ionic strength (*e.g.*100 mmol/L). Under higher ionic strength solutions, the quantity of positive and negative ions would increase to large scale, so the competitive binding of positive ion (Na^+) to aptamer and negative ion (Cl^-) to CV molecule had occurred, which would decrease the electrostatic attraction between CV molecule and Ars-3 aptamer to some extent.

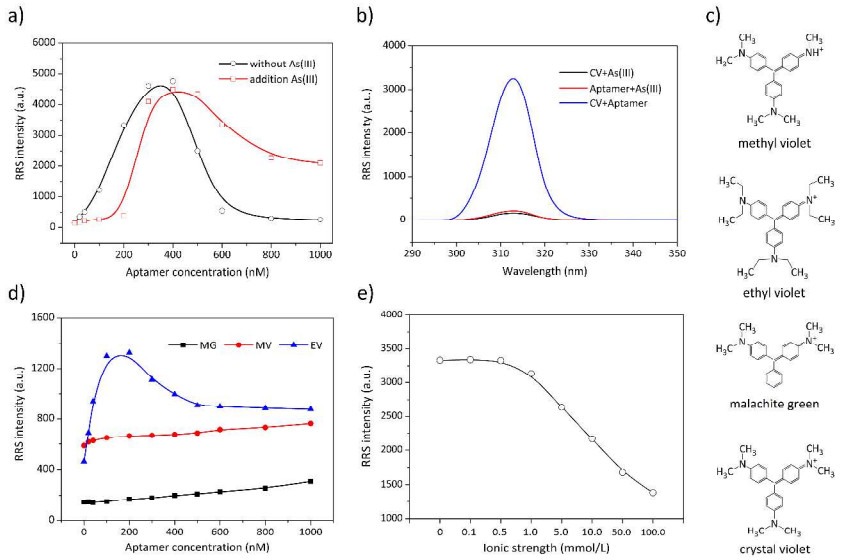

Fig. 1 (a) RRS intensities of CV solutions treated with varying concentration of Ars-3 aptamer and 100 ppb of As(III) for 20 min. (b) RRS spectra of the solutions containing different substance. (c) Chemical structure of cationic TPM dyes in this study. (d) RRS intensities of other cationic TPM dyes (*e.g.* MG, MV and EV) solutions treated with varying concentration of Ars-3 aptamer for 20 min. The concentrations of cationic TPM dyes were 100 μM. (e) RRS intensities of CV solutions treated with 200 nM of Ars-3 aptamer under different ionic strength for 20 min.

3.2 Interactions between nanoparticles and arsenic(III)

Ars-3 aptamer had the high affinity to As(III) with a dissociation constant of 7.05 nM, so it may has a special effect on the above nanoparticles. To investigate the interactions between As(III) and nanoparticles, we added 100 ppb of As(III) into nanoparticles solutions, and the RRS intensity was recorded. As showed in Fig. 1(a), the RRS intensity of solutions before and after the addition of As(III) was changed greatly. The introduction of As(III) decreased the RRS intensity of solutions when the concentration of aptamer was lower than 400 nM, while the RRS values incareased at higher concentration of aptamer.

Generally, the RRS intensity is associated with the size,

concentration and properties of particles in colloidal solutions, and its values will comply with Rayleigh Equation to some extent showed as follows:

$$I(R,\theta) = I_0 \frac{9\pi^2 \rho v^2}{2\lambda^4 R^2}\left[\frac{n_2^2 - n_1^2}{n_2^2 + 2n_1^2}\right]^2 \left(1+\cos^2\theta\right)$$

Where: I_0 and λ are the intensity and wavelength of excited light; ρ and v represent the density and volume of particles in solution; n_2 and n_1 refer to the refractive index of disperse phase and disperse medium, respectively; θ is a scattering angle; both π and R are constant.

The maximum RRS intensity had achieved at 310 nm of excited light in the preliminary experiments. According to Rayleigh Equation, the RRS intensity was depended largely on the size of particles under the same experimental conditions. Therefore, it can be deduced that the variation of RRS intensity in solutions was probably ascribed to the size alteration of nanoparticles caused by As(III).

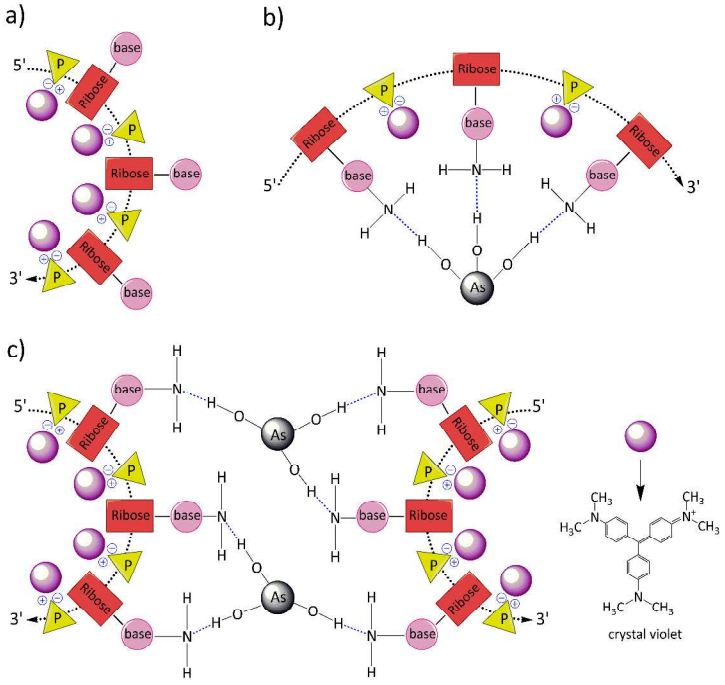

Scheme 2 Supposed principles of nanoparticles assembly and its interactions with arsenic. (a) Nanoparticles were assembled by CV and Ars-3 aptamer *via* the electrostatic force between positive charges of CV molecules and negative charges of phosphate backbone in DNAs. The size of nanoparticles was decreased and increased through the intramolecular (b) and intermolecular (c) hydrogen bonds between As(III) and bases of DNAs, respectively.

3.3 CD characterization of Ars-3 aptamer

Circular dichroism (CD) measurement is a powerful tool and usually used to investigate some biomolecules such as amino acid, peptides, proteins and nucleic acids. To deduce the interactions among aptamer, CV and As(III), the CD measurement was utilized to monitor the confirmation change of aptamer in the solutions. Fig. 2(a) shows the CD spectra of aptamer solutions treated with 100 ppb As(III). Ars-3 aptamer (generally B-DNA) has a negative peak at 240-260 nm and a positive peak at 270-290 nm, which is in accordance with previous reports.[23] After the addition of As(III), the value of negative and positive peaks were decreased, but the location of peaks did not change. This result indicated that As(III) could bind to Ars-3 aptamer, which interfered bases from the transition of strong π→π* with ribodesose, thus resulted in the decrease of CD peak. However, the introduction of CV had changed the position and peaks of Ars-3 aptamer. As showed in Fig. 2(b), the sharp negative at 220 nm and positive peaks at 320 nm were observed, which indicated that CV molecules and Ars-3 aptamer formed the CV-aptamer complexes (particles), thus the original conformation of aptamer might changed. In this case, the addition of As(III) decreased the CD peaks due to its high affinity to Ars-3 aptamer.

3.4 PCS analysis of nanoparticles

According to Rayleigh Equation, the RRS intensity is associated with the nanoparticles size in solutions. Herein, the average size of nanaoparticles was determined by PCS analysis throughout the experiments, and the result is showed in Table 1. With increasing number of Ars-3 aptamer, the average diameter of particles decreased significantly. At lower concentration of aptamer (lower than 200 nM), the diameter of particles was close to 1 μm, which was larger than the wavelength of excited light (310 nm). Once the particle diameter exceed excited wavelength, some energy of excitation would lose by reflection and caused the lower RRS intensity. The present result shows that the RRS intensity attained the maximum value at 400 nM of Ars-3 aptamer (Fig. 1(a)), where the particle diameter is about 80 nm. When the diameter of particles is larger than 100 nm, the reflection and refraction of excited light in the some parts of particles will happen, thus lead to the decrease of RRS intensity, which can partially explain why the RRS values at 200 nM and 300 nM of aptamer were lower than that at 400 nM of aptamer.

The electrostatic repulsion among aptamers and its competitive

binding to CV molecules could account for the difference size of nanoparticles. Under higher concentration of aptamer (e.g. 600 nM or 800 nM), the available aptamer for binding to CV molecules increased in large scale, but the amount of CV molecules did not raise, so the competitive binding occurred inevitably, which would prevent aptamers from binding or absorbing massive CV molecules to assemble large particles. Moreover, the electrostatic repulsion among aptamers also prevented nanoparticles from aggregating together.

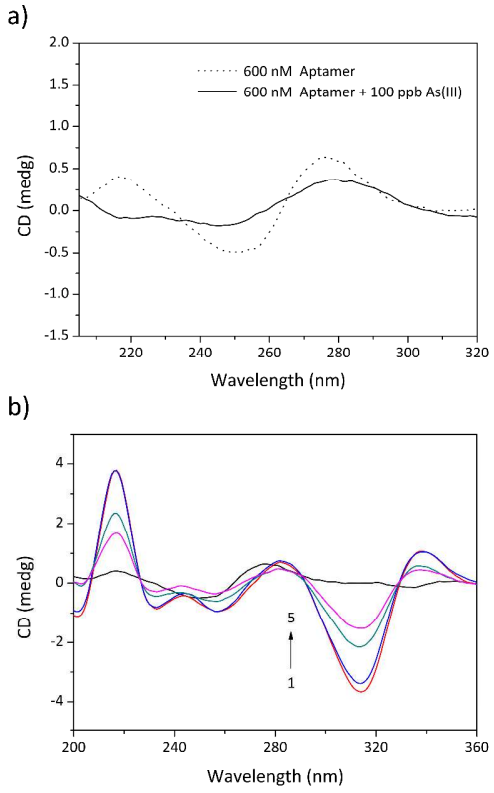

Fig. 2 CD spectra of Ars-3 aptamer distributed in different solutions. (a) Aptamer was presented in the 100 ppb of As(III). (b) Nanoparticles assembled by 600 nM aptamer and 100 μM CV was treated with varying concentration of As(III). Numbers 1 to 4 refer to 0, 1, 40 and 100 ppb of As(III), respectively. Number 5 represents the CD spectra of Ars-3 aptamer distributed solely in 50 mM HEPS buffer (pH 7.2).

In addition, the results in Table 1 indeed confirmed that the addition of As(III) caused the size alteration of nanoparticles. Under lower concentration of aptamers (lower than 200 nM), the particles diameter was decreased gradually after the addition of 100 ppb As(III), which lead to the decrease in RRS intensity at 310 nm. The maximum decline ratio of RRS intensity was about 7.4 fold, where the nanoparticles were assembled by 200 nM aptamer and 100 μM CV solutions. In this case, the average size of nanoparticles had also decreased from 273 nm to 168 nm. However, the variation trend of nanoparticles diameter was opposite at higher concentration of aptamers. The RRS intensity of solutions had enhanced obviously after the addition of As(III), especially its values at least increased by 6-fold when the concentration of aptamer was over 600 nM in the assembly of nanoparticles. Accordingly, the average diameter of nanoparticles had increased from 28.7 nm to 73 nm.

The reasons for above two opposite size variation trend may lie in the different properties between large and small nanoparticles. The large nanoparticles were assembled at lower concentration of aptamers, where a large number of CV molecules or its micelle structure might be enclosed by a single aptamer molecule. The whole large nanoparticle was loose and full with holes due to the electrostatic repulsion of CV molecules, which enable As(III) insert easily into the inner parts of nanoparticle. Because arsenite contains three hydroxy group (-OH) in aqueous solutions, it would shorten the distance of neighboring bases and compact the whole nanoparticles through strong hydrogen bonds between -OH of As(III) and $-NH_2$ of bases in DNAs, just as showed in Scheme 2(b). In this case, the intramolecular hydrogen bonds would play a leading role in maintaining the whole nanoparticles. As a result, the size of large nanoparticles was ultimately decreased by the addition of As(III). In the case of higher concentration of aptamers, the small nanoparticles with tight structure would be assembled. Because the available aptamers had increased in large scale, the quantity of small nanoparticles in solutions would be far more than that of large nanoparticles. Therefore, the introduction of As(III) would bind to these small nanoparticles and aggregate them *via* strong intermolecular hydrogen bonds between As(III) and aptamers (Scheme 2(c)), which had caused the significant increase in the average size of particles.

Table 1 Average size and RRS intensity variation of nanoparticles.

Aptamer (nM)	PDI†	Mean size (nm)		RRS intensity increased (fold)
		Without As(III)	With As(III)‡	
0	none*	none	none	-0.06
20	0.320	872.0	602.5	-1.08
40	0.313	1213.0	956.9	-1.27
100	0.391	908.8	586.9	-3.59
200	0.273	273.2	168.2	-7.40
300	0.240	142.0	153.6	-0.13
400	0.236	79.37	92.03	-0.06
500	0.258	59.53	86.48	0.74
600	0.212	28.71	72.97	6.04
800	none	none	none	6.66
1000	none	none	none	6.98

† PDI indicates the dispersion degree of solutions. The lower value of PDI means that particles distributed evenly in solutions.

‡ Final concentration of As(III) in solution was 100 ppb.

* Here "none" represents the value did not calculated by PCS machine due to the instability of the solution.

3.5 SPM observation of nanoparticles

To further confirm the assembly of nanoparticles and its size alteration caused by As(III), the CV solutions treated with Ars-3 aptamers and As(III) were characterized by SPM , and their images are showed in Fig. 3. In the absence of aptamer, some CV molecules clustered together due to hydrophobic interaction, and some of them had formed particles with average diameter of 10 nm (Fig. 3(a)). The shape of Ars-3 aptamer was a linear chain and it distributed evenly in the solutions (Fig. 3(b)). The addition of As(III) had changed the shape of DNAs to some extent. Some aptamers interacted with As(III) to form irregular particles (Fig. 3(c)), which was an evidence for the high affinity of Ars-3 aptamer to As(III). It could be clearly observed that the nanoparticles were indeed assembled by CV molecules and Ars-3 aptamer, but the shape and size of them were changed greatly under different concentration of aptamer. As showed in Fig. 3(d),

some spherical nanoparticles with diameter in a range from 200 nm to 300 nm were assembled under 200 nM of Ars-3 aptamer. Although the size of nanoparticles decreased significantly to 30 nm at 600 nM of aptamers, the numbers of them had increased obviously (Fig. 3(e)). In the case of 800 nM aptamers, a great number of small nanoparticles had deposited on the surface of mica sheet to form a flat film, as showed in Fig. 3(f). In the presence of 100 ppb of As(III), the size of large and small nanoparticles decreased and increased respectively (Fig. 3(g~h)), which were in accordance with the results of PCS analysis. As showed in Fig. 3(i), the film on mica sheet looked more compacted than before, which indicated that the addition of As(III) could stabilize nanoparticles.

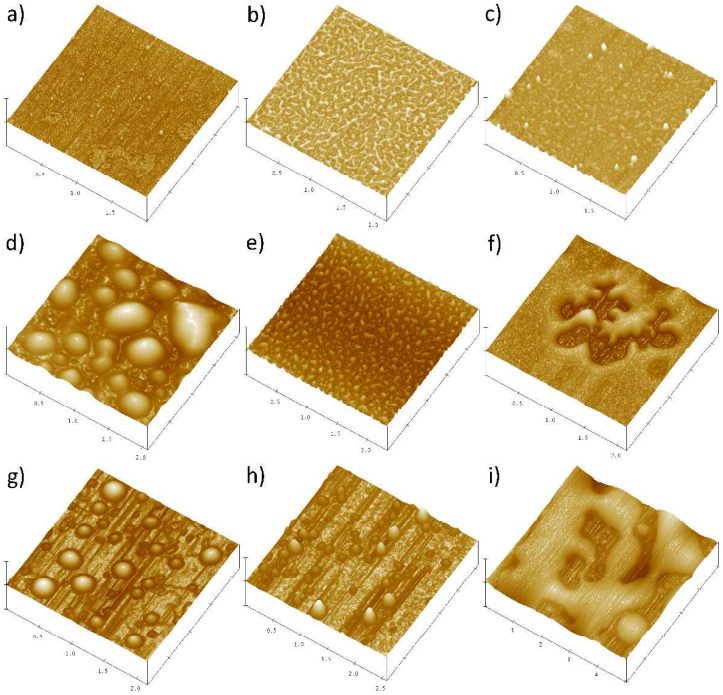

Fig. 3 Scanning probe microscope (SPM) observation of solutions containing: (a) 100 μM CV solution; (b) 600 nM Ars-3 aptamer solutions; (c) sample b + 1000 ppb of As(III); (d~f) nanoparticles assembled by 100 μM CV as well as 200 nM, 600 nM and 800 nM of Ars-3 aptamer, respectively; (g~i) samples (d~f) + 100 ppb of As(III).

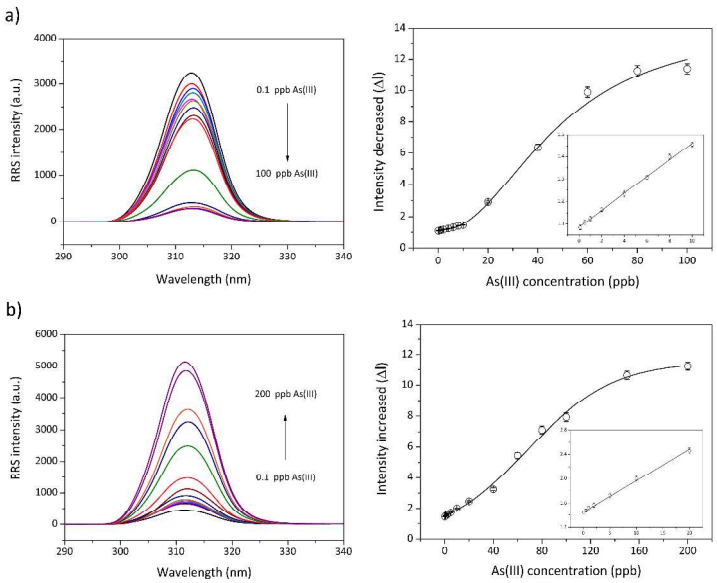

Fig. 4 Sensitivity of the biosensor for As(III) detection in aqueous solution. (a) RRS spectra (left) and calibration curve (right) of biosensor-200 responded to 0, 0.1, 0.5, 1, 2, 4, 6, 8, 10, 20, 40, 60, 80 and 100 ppb As(III). The curve was fitted to Hill plot with a correlation coefficient of 0.973. Inset: RRS intensity decreased value at low As(III) concentrations. The liner regression equation was y = 0.037 x + 1.086, with a correlation coefficient of 0.998. (b) RRS spectra (left) and calibration curve (right) of biosensor-600 treated with 0, 0.1, 0.5, 1, 2, 5, 10, 20, 40, 60, 80, 100, 150 and 200 ppb As(III). The curve was fitted to Hill plot with a correlation coefficient of 0.989. Inset: RRS intensity increased value at low As(III) concentrations. The liner regression equation was y = 0.051 x + 1.453, with a correlation coefficient of 0.997.

3.6 Sensitivity of the biosensor for arsenic(III) detection

According to above results, the addition of 100 ppb As(III) had caused the maximum decline and increase ratio of RRS intensity in the two different nanoparticles, which were assembled under 200 nM and 600 nM of Ars-3 aptamer, respectively. Thus these two kinds of nanoparticles, referring to biosensor-200 and biosensor-600 in the subsequent experiments, can be used as the powerful tools to detect As(III) in aqueous solution.

To test the performance of the biosensor-200, the system was treated with varying concentration of As(III) from 0.1 ppb to 100 ppb, and the RRS intensity at 310 nm was recorded. As shown in Fig. 4(a), the RRS intensity decreased greatly with the increasing concentration of As(III), especially higher concentrations of As(III) caused a sharp decline of signal. Interestingly, the average size of nanoparticles had decreased from 273 nm to 168 nm (Table 1), which demonstrated that the variation of RRS intensity was depended largely on the size alteration of nanoparticles caused by the addition of As(III). To quantify As(III) in solution, the RRS intensity of biosensor-200 are plotted, and the calibration curve looks like a sigmoid shape, which was fitted to Hill plot with a correlation coefficient of 0.973. The RRS intensity at low As(III) concentrations was fitted to linear with a correlation coefficient of 0.998. Based on the previous reports,[23, 28, 35] 3σ/slope was used to determine the detection limit of biosensor-200 as 0.3 ppb, which is lower than U.S. EPA and WHO defined toxicity level of arsenic in drinking water (10 ppb). The similar method was also employed to determine the detection limit of biosensor-600 as 0.2 ppb and a dynamic range up to 200 ppb (Fig. 4(b)), where the RRS intensity enhanced obviously with the increasing concentration of As(III). The above results indicate that these nanoparticles indeed possesses the potential application of detecting As(III) sensitively in aqueous solution.

3.7 Selectivity of the biosensor for arsenic(III) detection

The selectivity of the biosensor for As(III) detection was also investigated. A variety of analogues of As(III) and competing metal ions, including methyl arsenic acid (MMA), dimethyl arsenic acid (DMA), As(V), Sb(III), Bi(III), Pb(II), Cd(II), Hg(II), Ag(I), Mg(II), Zn(II), Mn(II), Ni(II), Cu(II) , Fe(II), Fe(III) and Ca(II), were individually exposed to biosensor-200 and the RRS intensity were monitored. Fig. 5 shows the difference in RRS intensity decrease among blank and solutions containing 10 ppb of As(III) and other metal ions. The results demonstrate that all the other metal ions display slight and negligible interferences on biosensor-200 for As(III) detection.

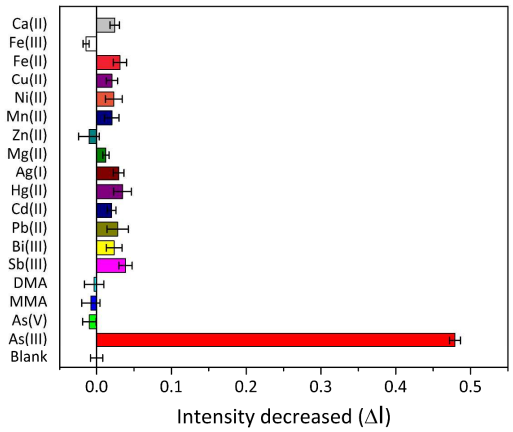

Fig. 5 Selectivity of the biosensor-200 for As(III) detection in aqueous solution. The concentrations of metal ions were 10 ppb.

3.8 Detection of arsenic(III) in water samples

The application of present biosensor based on RRS assay was evaluated for the determination of As(III) in several water samples containing different concentrations of As(III) and some other metal cations and anions. The results are summarized in Table 2, which displays that the mean recovery of samples was in the range of 96.7-104% and the relative standard deviation (RSD) were between 5.2% and 10.8%. The results reveal the potential application of present biosensor for As(III) detection in water samples.

Table 2 Determination of As(III) in water samples.

Water samples	Biosensor-200			Biosensor-600		
	Mean found (ppb)	Recovery (%)	RSD (%)	Mean found (ppb)	Recovery (%)	RSD (%)
As^{III}(1)†, As^{V}(2), MMA(1), Pb^{II}(1), Cd^{II}(2), Fe^{II}(1), Mn^{II}(2), NO_3^- (6), SO_4^{2-} (3)	1.02 ± 0.11	102	10.8	0.98 ± 0.09	98	9.2
As^{III} (6), DMA(5), MMA(4), Hg^{II}(5), Cd^{II}(6), Mg^{II}(7), Ag^{I}(6), Ca^{II}(1), NO_3^- (28), SO_4^{2-} (7), Cl^- (2)	5.80 ± 0.30	96.7	5.2	5.83 ± 0.59	97.2	10.1
As^{III} (10), As^{V}(9), DMA(10), Pb^{II}(8), Ni^{II}(2), Cu^{II}(6), Zn^{II}(7), NO_3^- (16), SO_4^{2-} (8) , Cl^- (14)	9.77 ± 0.81	97.7	8.3	10.4 ± 0.85	104	8.2

† Final concentration (ppb) of ions was added.

4. Conclusions

In conclusion, we have successfully assembled a variety of nanoparticles with different size *via* controlling the concentration of Ars-3 aptamer in CV solutions. The large nanoparticles were assembled by lower concentration of aptamers and CV molecules, while the small nanoparticles were constructed under higher concentration of aptamers due to electrostatic repulsion among aptamers and its competitive binding to CV molecules. We also discovered that the introduction of As(III) could change the size of nanoparticles, thus caused the variation of RRS intensity. In the presence of As(III), the maximum decline ratio of RRS intensity was achieved for large nanoparticles assembled at 200 nM of aptamers, where their average size had decreased from 273

nm to 168 nm. In the case of small nanoparticles, the maximum increase ratio of RRS intensity was obtained when the concentration of aptamer was over 600 nM. Combined with a RRS spectral assay, we have successfully developed an effective biosensor for As(III) detection using above two kinds of nanoparticles as target recognition element. The detection limit of our approach is about 0.2 ppb, which is about two orders lower than U.S. EPA and WHO defined toxicity level of arsenic in drinking water. The present biosensor also displayed high selectivity over other competitive metal ions, with an excellent recovery in the detection of real water samples. The experimental results reported here exhibit that the biosensor will provide the reliable, highly sensitive and selective monitoring method for arsenic in environmental and other applications.

Acknowledgements

This work was supported by the National Natural Science Foundation of China (21205020, 31071860), the National High-Tech Research and Development Plan (2012AA101405), the Special Fund for Agro-scientific Research in the Public Interest of China (200903056), and the Innovation Fund of Shanghai Jiao Tong University for Postgraduate.

References

1. S. Fendorf, H. A. Michael and A. van Geen, *Science*, 2010, **328**, 1123-1127.
2. A. A. Ensafi, A. C. Ring and I. Fritsch, *Electroanal*, 2010, **22**, 1175-1185.
3. B. K. Jena and C. R. Raj, *Anal Chem*, 2008, **80**, 4836-4844.
4. V. C. Ezeh and T. C. Harrop, *Inorg Chem*, 2012, **51**, 1213-1215.
5. D. E. Mays and A. Hussam, *Anal Chim Acta*, 2009, **646**, 6-16.
6. K. A. Francesconi and D. Kuehnelt, *Analyst*, 2004, **129**, 373-395.
7. M. Berg, P. T. K. Trang, P. H. Viet, N. Van Mui and J. R. Van Der Meer, *Environ Sci Technol*, 2005, **39**, 7625-7630.
8. J. R. Kalluri, T. Arbneshi, S. A. Khan, A. Neely, P. Candice, B. Varisli, M. Washington, S. McAfee, B. Robinson, S. Banerjee, A. K. Singh, D. Senapati and P. C. Ray, *Angew Chem Int Edit*, 2009, **48**, 9668-9671.
9. K. de Mora, N. Joshi, B. L. Balint, F. B. Ward, A. Elfick and C. E. French, *Anal Bioanal Chem*, 2011, **400**, 1031-1039.
10. X. X. Wang, Y. Lv and X. D. Hou, *Talanta*, 2011, **84**, 382-386.
11. M. Famulok, J. S. Hartig and G. Mayer, *Chem Rev*, 2007, **107**, 3715-3743.
12. I. Willner, B. Shlyahovsky, M. Zayats and B. Willner, *Chem Soc Rev*, 2008, **37**, 1153-1165.
13. J. W. Liu, Z. H. Cao and Y. Lu, *Chem Rev*, 2009, **109**, 1948-1998.
14. U. Rant, K. Arinaga, S. Scherer, E. Pringsheim, S. Fujita, N. Yokoyama, M. Tornow and G. Abstreiter, *P Natl Acad Sci USA*, 2007, **104**, 17364-17369.
15. H. Shi, X. X. He, K. M. Wang, X. Wu, X. S. Ye, Q. P. Guo, W. H. Tan, Z. H. Qing, X. H. Yang and B. Zhou, *P Natl Acad Sci USA*, 2011, **108**, 3900-3905.
16. T. Chen, M. I. Shukoor, Y. Chen, Q. Yuan, Z. Zhu, Z. Zhao, B. Gulbakan and W. Tan, *Nanoscale*, 2011, **3**, 546-556.
17. R. M. Kong, X. B. Zhang, Z. Chen and W. Tan, *Small*, 2011, **7**, 2428-2436.
18. X. He, L. Hai, J. Su, K. Wang and X. Wu, *Nanoscale*, 2011, **3**, 2936-2942.
19. Y. R. Wu, K. Sefah, H. P. Liu, R. W. Wang and W. H. Tan, *P Natl Acad Sci USA*, 2010, **107**, 5-10.
20. M. Hollenstein, C. Hipolito, C. Lam, D. Dietrich and D. M. Perrin, *Angew Chem Int Edit*, 2008, **47**, 4346-4350.
21. Y. Xiang, A. J. Tong and Y. Lu, *J Am Chem Soc*, 2009, **131**, 15352-15357.
22. J. W. Liu, A. K. Brown, X. L. Meng, D. M. Cropek, J. D. Istok, D. B. Watson and Y. Lu, *P Natl Acad Sci USA*, 2007, **104**, 2056-2061.
23. Y. Wu, S. Zhan, F. Wang, L. He, W. Zhi and P. Zhou, *Chem Commun*, 2012, **48**, 4459-4461.
24. Z. Jiang, Y. Fan, M. Chen, A. Liang, X. Liao, G. Wen, X. Shen, X. He, H. Pan and H. Jiang, *Anal Chem*, 2009, **81**, 5439-5445.
25. Z. Jiang, G. Wen, Y. Fan, C. Jiang, Q. Liu, Z. Huang and A. Liang, *Talanta*, 2010, **80**, 1287-1291.
26. Z. Jiang, L. Zhou and A. Liang, *Chem Commun*, 2011, **47**, 3162-3164.
27. A. Liang, Y. Zhang, Y. Fan, C. Chen, G. Wen, Q. Liu, C. Kang and Z. Jiang, *Nanoscale*, 2011, **3**, 3178-3184.
28. Y. Wu, S. Zhan, L. Xu, W. Shi, T. Xi, X. Zhan and P. Zhou, *Chem Commun*, 2011, **47**, 6027-6029.
29. H. Q. Luo, N. B. Li and S. P. Liu, *Biosens Bioelectron*, 2006, **21**, 1186-1194.
30. D. M. Kolpashchikov, *J Am Chem Soc*, 2005, **127**, 12442-12443.
31. R. Y. Tsien, J. R. Babendure and S. R. Adams, *J Am Chem Soc*, 2003, **125**, 14716-14717.
32. A. C. Bhasikuttan, J. Mohanty, W. M. Nau and H. Pal, *Angew Chem Int Edit*, 2007, **46**, 4120-4122.
33. D. M. Kong, Y. E. Ma, J. Wu and H. X. Shen, *Chem-Eur J*, 2009, **15**, 901-909.
34. M. Kim, H. J. Um, S. Bang, S. H. Lee, S. J. Oh, J. H. Han, K. W. Kim, J. Min and Y. H. Kim, *Environ Sci Technol*, 2009, **43**, 9335-9340.
35. Y. Wu, L. Liu, S. Zhan, F. Wang and P. Zhou, *Analyst*, 2012, **137**, 4171-4178.

A table of contents entry

Manuscript ID: NR-ART-06-2012-031418

Title: Nanoparticles assembled by aptamers and crystal violet for arsenic(III) detection in aqueous solution based on a Resonance Rayleigh scattering spectral assay

Text:

Arsenic binding aptamers and cationic dyes were used to assemble functional nanoparticles for As(III) detection based on size alteration

Color graphic: